Note: This copy is for your personal non-commercial use only. To order presentation-ready copies for distribution to your colleagues or clients, contact us at www.rsna.org/rsnarights.

Radiology

Reviving the Dinosaur: Virtual Reconstruction and Three-dimensional Printing of a Dinosaur Vertebra[1]

René Schilling, MD
Benjamin Jastram, Dipl-Ing
Oliver Wings, Dr rer nat
Daniela Schwarz-Wings, Dr rer nat
Ahi Sema Issever, MD

Purpose: To demonstrate the feasibility of using computed tomography (CT) to confirm the identity of an unprepared fossil and to use the CT dataset to separate the fossilized bone from its surrounding sediment matrix and produce a three-dimensional (3D) print.

Materials and Methods: The examined object was a plaster jacket containing an unprepared fossil. CT was performed with a 320-section multidetector unit. A marching cube–based method was used to transform the voxel CT dataset into triangle-based, editable geometry. Then, a comprehensive postprocessing step was performed to isolate the geometry of the vertebra from its surrounding fossilized matrix. Finally, the resulting polygon mesh describing only the vertebra was used for a physical 3D reconstruction by using a selective laser sintering machine.

Results: The CT examination provided enough data to assign the fossil to the genus *Plateosaurus*. In addition, much valuable information about the fossil has been gained—in particular the visualization of multiple fractures and the destruction of the anterior rim of the vertebral body. Finally, the results show that the 3D print generated, including the fractures and the anterior destruction, may be considered an accurate copy of the bone with the unprepared fossil.

Conclusion: The authors demonstrated the feasibility and potential utility of combining CT with 3D printing, providing a nondestructive method to future paleontologists.

©RSNA, 2013

[1] From the Department of Radiology, Charité Campus Mitte, Universitaetsmedizin Berlin, Charitéplatz 1, 10117 Berlin, Germany (R.S., A.S.I.); 3D Laboratory, Faculty II, Institute for Mathematics, Technische Universitaet Berlin, Berlin, Germany (B.J.); and Museum of Natural History, Leibniz Institute for Evolution and Biodiversity Research, Berlin, Germany (O.W., D.S.W.). Received April 1, 2013; revision requested May 3; revision received July 17; accepted August 6; final version accepted September 4. **Address correspondence to** A.S.I. (e-mail: *ahi-sema.issever@charite.de*).

©RSNA, 2013

From 1909 through 1913, one of the most successful dinosaur excavations took place in the territory of today's Tanzania (1). Two German paleontologists, Janensch and Hennig, were commissioned by the Museum für Naturkunde (Museum of Natural History, Berlin, Germany) to lead an excavation in the Jurassic strata near Tendaguru Hill. The yield of their expedition was awe inspiring; about 235 tons of fossil bones were excavated and transported to Berlin. One of the spectacular dinosaur skeletons reconstructed, exhibited in the Museum für Naturkunde, is the skeleton of *Brachiosaurus brancai*, which, at a height of 13.27 m, is the world's largest mounted dinosaur skeleton to date.

In the same year that Janensch and Hennig started the German Tendaguru expedition, employees of a brick manufacturer found large fossil skeletal remains in a clay pit south of Halberstadt (Sachsen-Anhalt, Germany). The fossil collector and dentist in Halberstadt, Troger, was informed, and he contacted Jaekel, a paleontologist from Greifswald, Germany, asking him to evaluate the findings. Jaekel quickly realized the uniqueness of the finds and initiated their appropriate excavation (2). From 1910 to 1923, remains of more than 50 individuals of the dinosaur *Plateosaurus* (Fig 1) were dug out. Among the large number of finds were several partial and well-preserved skeletons, which were given field numbers under the charge of Jaekel. Interestingly, Janensch—one of the leading scientists in the Tendaguru excavation—later also became involved in the excavations in Halberstadt. Final excavations between 1923 and 1927 yielded another four partial skeletons, which were labeled from A to D under the direction of Janensch and his preparator Siegert, his technical assistant who specialized in fossil handling, preparation, and conservation (2). After 1927, the Museum für Naturkunde took over most of the material that had been excavated in Halberstadt, and most of the *Plateosaurus* material was then stored together with fossils from Tendaguru. However, because fossils are often brittle and fragile, they were protected by jackets made of plaster of paris and burlap strips before they were transported.

Nearly 2 decades after the arrival of these plaster jackets in the Museum für Naturkunde, during the bombing of Berlin in World War II, a bomb hit the second floor of the museum's east wing, causing a chain reaction that ended with the collapse of the east wing into the museum's basement, where many unprepared fossils were stored. Many fossil bones and unprepared plaster jackets and/or their labels were destroyed; others were scattered and buried in rubble. The fact that different excavation projects used different or partially overlapping labeling systems for their findings made matters even more complicated. For findings of the German Tendaguru expedition, for example, letters indicated specific excavation locations, whereas in Halberstadt, each letter identified an individual dinosaur. Therefore—to this date—it has remained a major challenge to sort and identify some of the unprepared plaster jackets in the Museum für Naturkunde to reassign them to their origin. Fortunately, some of the detailed drawings (Fig 2) and protocols documenting every excavation have survived the war, but knowledge of what is inside the unprepared plaster jackets is ultimately essential for the identification process. The typical way of gaining knowledge about the inside of an unprepared fossil plaster jacket is by means of fossil preparation, including the removal of the plaster and all sediment surrounding the fossil plus restoration and conservation of the specimen. Preparation is thus a very time-consuming procedure that must be performed by highly skilled preparators. However, any conventional preparation may not only lead to a possible loss of remaining taphonomic and sedimentologic information of the find but can sometimes even destroy the fossil itself. Therefore, the nondestructive technique of computed tomography (CT), which was used as early as 1979 for the imaging of fossil bones (3), has become an invaluable tool in the field now known as paleoradiology.

In a joint study conducted by the Museum für Naturkunde, the 3D Laboratory of Technische Universitaet, and the Department of Radiology at the Charité Campus Mitte (all located in Berlin, Germany), we used CT to confirm the identity of an unprepared fossil. More important, however, the main objective of our joint study was to investigate the feasibility of virtually preparing the CT dataset to separate the fossilized bone from its surrounding sediment matrix and produce an actual three-dimensional (3D) print, which might serve as a model of the fossilized bone without preparation and destruction of taphonomic context. In other words, we performed this study to demonstrate the feasibility of using CT to confirm the identity of an unprepared fossil and to use the CT dataset to separate the fossilized bone from its surrounding sediment matrix and produce a 3D print.

Advance in Knowledge

- The feasibility of virtually preparing a CT dataset to separate fossilized bone from its surrounding sediment matrix and produce a three-dimensional print is shown.

Materials and Methods

Object and Excavation Drawing

The examined object from the collection of the Museum für Naturkunde

Published online before print
10.1148/radiol.13130666 **Content code:** CT

Radiology 2014; 270:864–871

Abbreviations:
ROI = region of interest
3D = three-dimensional

Author contributions:
Guarantors of integrity of entire study, R.S., B.J., O.W., A.S.I.; study concepts/study design or data acquisition or data analysis/interpretation, all authors; manuscript drafting or manuscript revision for important intellectual content, all authors; manuscript final version approval, all authors; literature research, all authors; statistical analysis, B.J.; and manuscript editing, all authors

Conflicts of interest are listed at the end of this article.

Figure 1

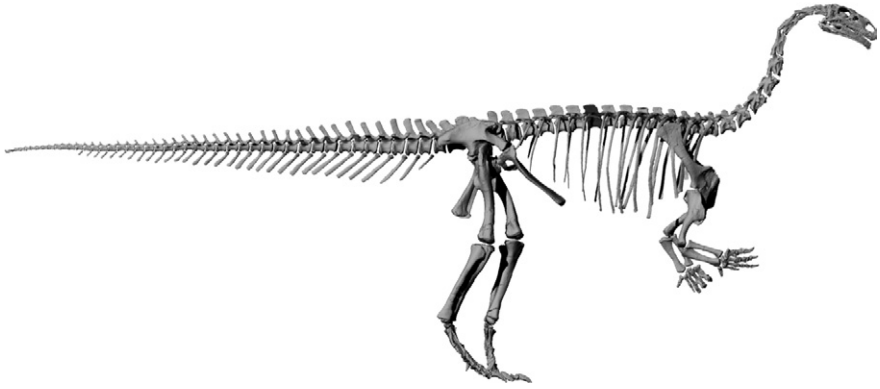

Figure 1: Illustration of *Plateosaurus* skeleton.

Figure 2

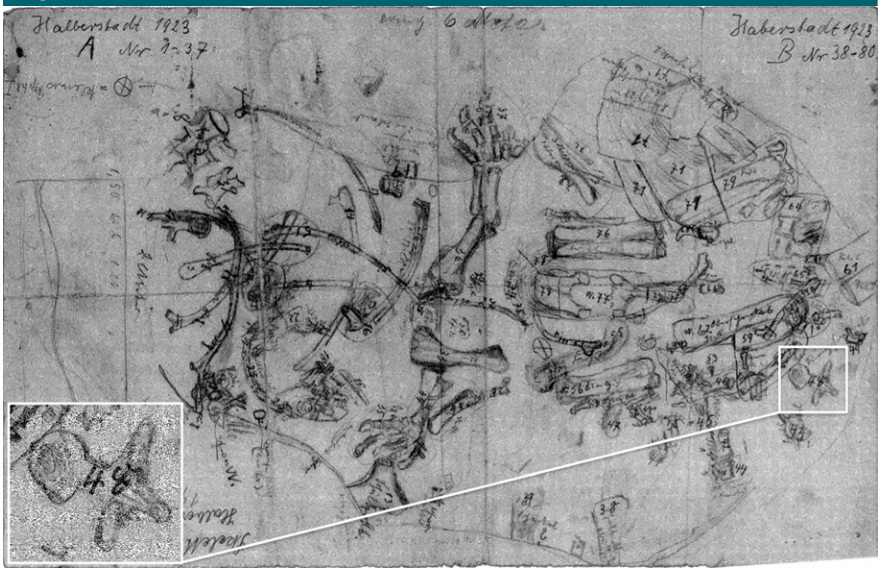

Figure 2: Digitized image of original excavation field map from Halberstadt, 1923. Inset is magnification of fossilized vertebra.

was a plaster jacket containing an unprepared fossil. It was 20 cm long and 15 cm high and weighed 5 kg. From its location within the collapsed basement of the museum, after the war it was assumed that the object would most likely belong to Tendaguru material from locality A and was therefore relabeled accordingly as A-48. To conserve the original 90-year-old plaster jacket and because it represents a quicker way of gaining insight into the specimen than preparation, in 2011 it was decided to use nondestructive CT for final verification of this relabeling.

Imaging

CT of the object was performed with a 320-section multidetector CT unit (Aquillion ONE; Toshiba, Otawara, Japan). A helical scan mode with a rotation time of 1.0 second was chosen. The tube voltage was set to 135 kVp, and a tube current of 450 mA was used. The field of view covered 23.3 cm, and the matrix size was 512 × 512 pixels, yielding an in-plane pixel size of 455 μm. Axial images (n = 1001) were acquired with a section thickness of 500 μm; subsequently, secondary multiplanar reconstructions were calculated in axial, coronal, and sagittal orientations, each with a section thickness of 3 mm.

Image Analysis

To examine the inner structure of the object at first all axial, coronal, and sagittal reconstructions were viewed with a full dynamic range of the window level and window width (Figs 3, *A*, 4, *A*, 4, *C*). Please note that the terms *axial, coronal,* and *sagittal* refer to the positioning and orientation of the fossil within the scanner and not to the anatomic orientation. To obtain an estimate of the size of the vertebral body within the two-dimensional original CT dataset, the distance between the anterior rim of the vertebral body and the tip of the spinosus process (length), the distance between the two ends of the left and right transversus processes (width), and the distance between the upper and lower endplate of the vertebral body (height) were measured (in centimeters). Next, a representative axial section was selected for measuring the attenuation values (in Hounsfield units) in the fossilized bone, the fossilized sediment matrix, and the surrounding protective plaster jacket (see circular regions of interest [ROIs] in Fig 3, *A*). To increase the visual differentiation between fossilized bone and fossilized sediment matrix, we deviated from the settings for optimal fossil demonstration proposed by Golder and Christian (4) (window level, 2640 HU; window width, 1040 HU) and set the window level and window width to 2600 HU (Fig 3, *B*). Image analysis was performed by using the open-source Digital Imaging and Communications in Medicine viewer and imaging software (OsiriX v.5.5; Pixmeo, Bernex, Switzerland) (R.S. and A.S.I., with 5 and 8 years of radiology experience, respectively).

Segmentation for the 3D Print

Herein, segmentation describes the process of computing a geometric and

Figure 3

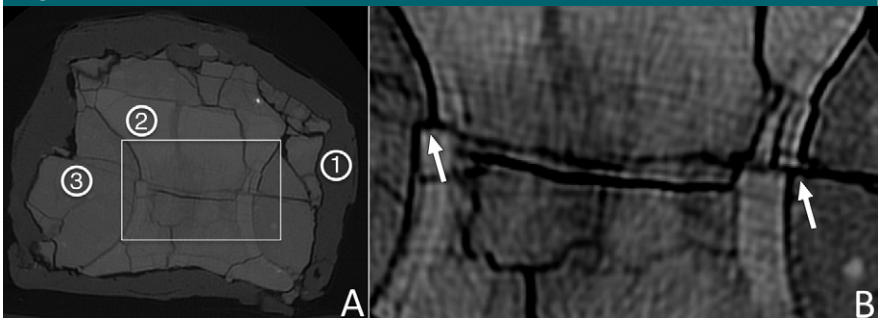

Figure 3: Axial CT scans of fossil. *A*, CT scan (window level, 4698 HU; window width, 13 493 HU) covers full scale of attenuation and depicts entire inner structure of scanned object, including surrounding plaster jacket, sediment matrix, and fossilized vertebral body. To obtain representative attenuation measurements, circular ROIs were placed in surrounding protective plaster (*1*), body of vertebra (*2*), and surrounding fossilized sediment matrix (*3*). *B*, To increase contrast between fossilized vertebral body and fossilized surrounding sediment matrix, a section—square in *A*—is depicted with window level of 2600 HU and window width of 2600 HU. Arrows in *B* indicate displacement of ventral and dorsal halves of vertebra (see arrows in Fig 6, *F*).

Figure 4

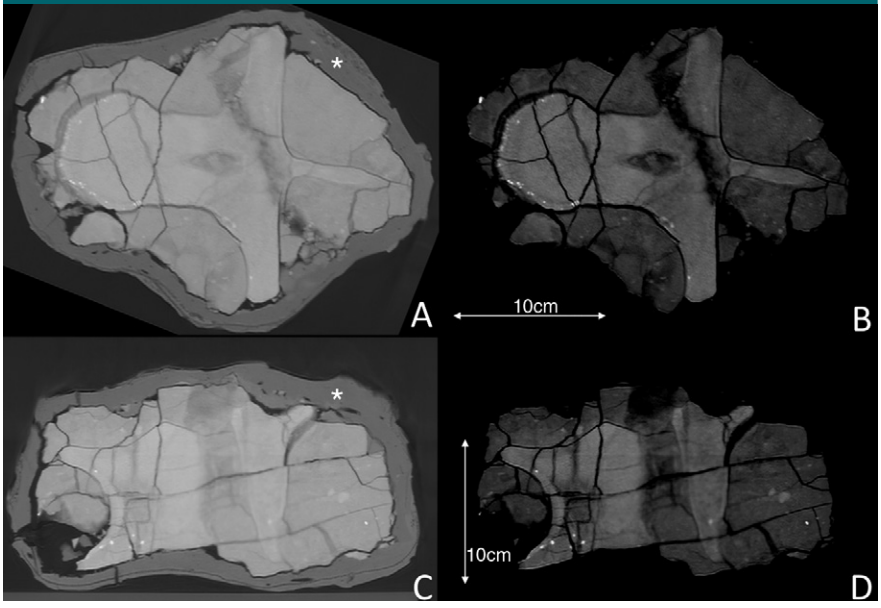

Figure 4: *A, B,* Coronal and, *C, D,* sagittal reconstructions of fossil with different window levels and widths. In *A* and *C*, window levels and widths were set to a full dynamic range (*A:* window level = 1370 HU, window width = 6836 HU; *C*: window level = 1113 HU, window width = 6322 HU). In *B* and *D*, the window level and width were set to 2600 HU. ∗ indicates surrounding hard plaster. Numerous fracture lines passing through fossil are clearly visible.

physically coherent object from a large and complex CT dataset by using specified thresholds. By defining thresholds for the attenuation values, algorithms isolate a specific pixel or voxel. The criteria of homogeneous selection ensure the segmentation of an interrelated two-dimensional or 3D object.

The given attenuation values of the CT dataset were the basis for building a 3D grid. Each grid cell contained a voxel. The transmission value of each voxel equaled the 8–16-bit value of its corresponding pixel in its specific section. To meet the definition of a voxel-based volume dataset, the axial dimensions of the grid cells needed to be equalized to form an isolinear grid. The smallest voxel size, in this case 500 μm, was used as the basis for correcting the other two axes to this value by interpolation.

Software (VolumeGraphicsStudio max 2.1; VGSmax, Heidelberg, Germany) was used for the digital reconstruction. At first, the attenuation values of the sections were transformed into a specific 16-bit domain represented by gray-scale values. The voxel with the highest linear attenuation coefficient was set to a value of 65 535. All attenuation values were represented in a histogram. The mapping of 256 gray-scale values to all attenuation values led to an insufficient accuracy in the visual selection of relevant structures. Therefore, the attenuation values had to be remapped into a smaller range to improve visual differentiation. Herein, remapping describes the process of selecting a narrow range within the whole 16-bit spectrum of attenuation values for a computer screen display. The reason for this method is the limited range of displayable gray values on a computer screen (8 bits, equaling 256 gray values). Therefore, by remapping these values it is possible to improve visual differentiation between heterogeneous structures. A 125 × 170 × 225 mm large ROI within the measurement volume was defined (by B.J., with 8 years of experience in additive manufacturing and 3D data analysis, preparation, and visualization). This narrowed down the attenuation values to the ROI domain (Fig 5, *A*). In the histogram, intervals were set to isolate the attenuation values that describe the fossil. However, because of the uncertainty of values (which means a high degree of similarity of attenuation values between the actual fossil and the surrounding sediment), the segmentation could not be automated and was based on visual inspection. Rewindowing and releveling of brightness and contrast values remarkably improved the ability to differentiate the fossilized

Figure 5

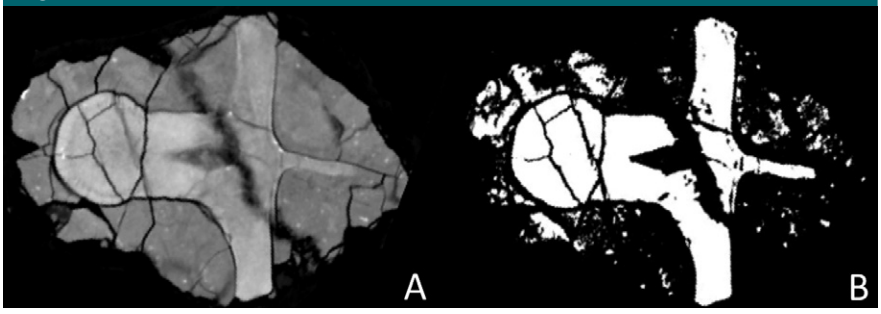

Figure 5: Coronal views of fossil. *A*, To segment the dataset for the 3D print and to improve visual differentiation, attenuation values were first remapped into a smaller range. *B*, Recalibration of brightness and contrast values further improves differentiation between fossilized vertebral body and its surrounding sediment matrix.

bone structures and surrounding stone material (Fig 5, *B*).

On the basis of the extracted dataset, an enveloping surface was generated. For triangle-based surface extraction, the marching cube algorithm was used.

An absolute precision of triangle edge length in geometric reconstruction of 340 μm (minimum) to 870 μm (maximum) per voxel was achieved. Overall, this value defines the raw level of detail. Further data improvements are interpolated and, therefore, metrologically not part of the original dataset.

Postprocessing for the 3D Print

Because of the similarities in the attenuation values, the extraction of the fossilized bone structure also led to the extraction of artifacts representing the surrounding fossilized sediment. A comprehensive postprocessing step was required to isolate the geometry that specifically describes the vertebra. Data processing software (ATOS; GOM, Braunschweig, Germany) was used to significantly reduce such artifacts and to perform basic mesh surface repair and noise-reduction operations. The process of surface extraction also generates unprintable artifacts such as free-floating surface conglomerates, single-sided detached surface patches, surface noise due to limitations in CT scan resolution, and holes in the triangle mesh. ATOS is a proprietary software package developed by GOM and is specifically used to actuate the company's optical 3D scanning systems ATOS I-III, Compact Scan, and Triple Scan and for processing the scan data. For postprocessing, this is a viable software solution because of the topologic similarities between surfaces extracted from optical and CT scan data.

3D Print Rapid Manufacturing

Finally, the postprocessed triangle mesh describing the vertebra was prepared for a physical 3D reconstruction. The 3D Laboratory of the Technische Universität Berlin Department of Mathematics operates a Formiga P100 selective laser sintering machine (EOS, Krailling, Germany) for manufacturing precise objects with high mechanical strength. The primary advantage of generative manufacturing methods is that it allows high variability of forms and structures, with a high level of detail and an extraordinary complexity of manufacturable objects, such as biologic structures like bones or molecules.

The selective laser sintering process is a layer-wise buildup of polyamide 12 powder. The focused laser beam melts the powder selectively layer by layer and thus connects the particles where the object should materialize physically in space. The precision in *x*-,*y*-, and *z*-axes is 100 μm. The minimal structural width of 400 μm in the *x*- and *y*-axes is defined by the laser focus width, and the minimal structural width in the *z*-axis is defined by the powder layer thickness of 100 μm. Considering the maximum resolution of the extracted geometry, the precision of the selective laser sintering process exceeds the scan data by an average factor of five.

Results

CT Scans

Figures 3–6 present different views of the scanned object with different window levels and widths. As expected from the general shape of the plaster jacket, it is apparent that the object consists of a fossilized vertebra and attached sedimentary matrix, which is surrounded by a plaster layer approximately 2.5 cm thick. Our images showed that the specimen actually is a *Plateosaurus* dorsal vertebra (see darkened vertebra in Fig 1), and further investigations revealed its location in the original field sketches from the Halberstadt excavation (Fig 2). It belongs to a series of associated bones excavated as two specimens, specimens A and B, which erroneously had been labeled with the letter A exclusively. The field number of the specimen is B-48, and the permanent collection number of the specimen in the Museum für Naturkunde is MB.R.5586.2.

Numerous fracture lines cross the sediment matrix and the embedded bone, and a major fracture zone (arrows in Fig 6, *F*) divides the vertebra, causing a slight displacement (arrows in Fig 3, *B*) of the ventral and dorsal halves. In the anterior part of the object, additional fracture lines that go through the surrounding plaster layer and extend into the fossil are visible (arrows in Fig 6, *A*, 6, *C*). Furthermore, in the sagittal reconstructions, a void between the surrounding plaster layer and the underlying fossil is apparent. The void contains multiple small bone fragments, suggesting that this portion of the fossil has been destroyed (Fig 6, *E*).

The measurements of the size of the vertebral body showed that the vertebral body has a length of 21.11 cm, a width of 17.78 cm, and a height of 8.74 m.

Attenuation measurement showed the surrounding plaster layer had the lowest attenuation (mean ± standard

Figure 6

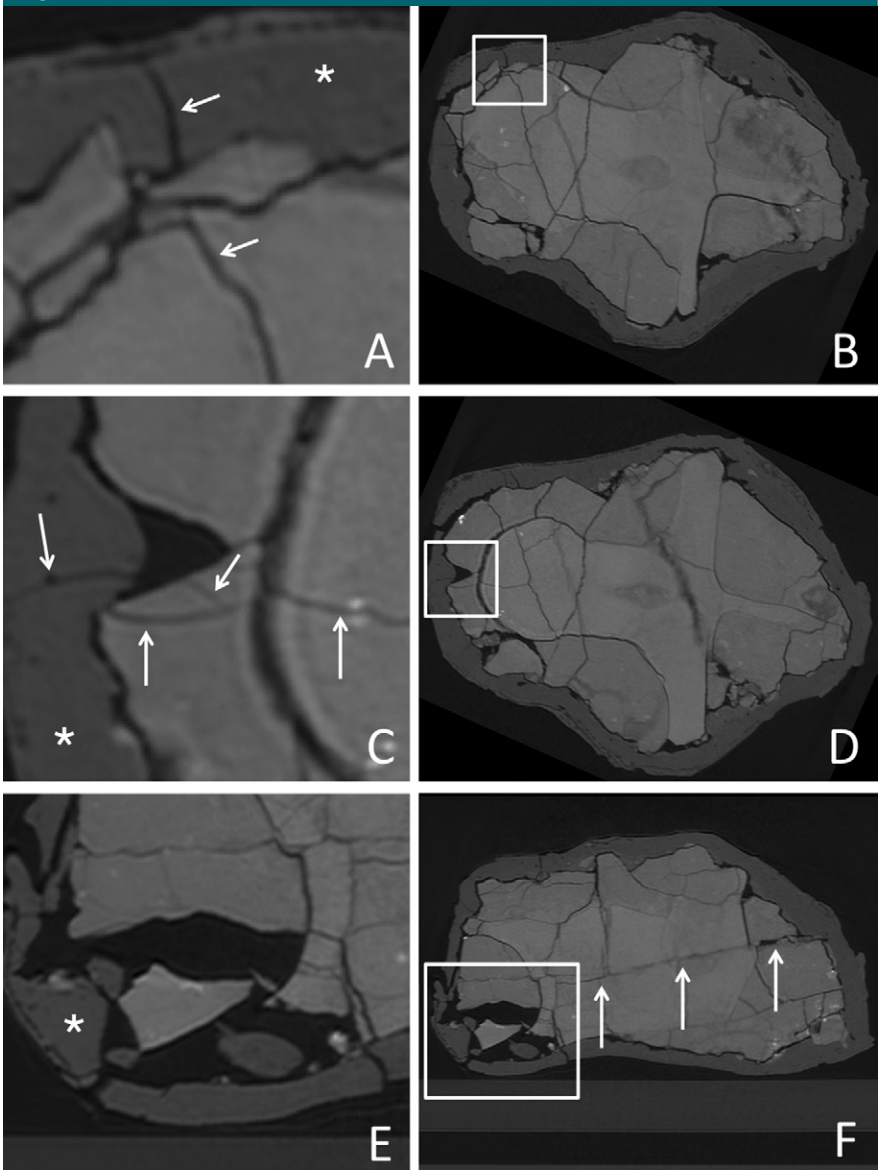

Figure 6: *A, C, E*, Enlarged sections of squares in *B*, *D*, and *F*, respectively. In coronal views (*A* and *C*), fracture lines (arrows) pass through surrounding plaster jacket (*) and extend into fossil. Arrows on sagittal view (*F*) mark major fracture zone that goes through entire fossil, causing displacement of ventral and dorsal halves as marked by arrows in Figure 3, *B*. In enlarged section of image (*E*), a void between the surrounding plaster (*) and the underlying—apparently destroyed—anterior part of fossil is clearly visible. Multiple small fragments can be identified within the void.

deviation, ~556 HU ± 76; see ROI 1 in Fig 3, *A*), whereas the fossilized bone had the highest attenuation (mean, ~2362 HU ± 102; see ROI 2 in Fig 3, *A*) followed by the fossilized sediment matrix (mean, 1896 HU ± 99; see ROI 3 in Fig 3, *A*).

3D Virtual Reconstruction and 3D Print

Figure 7 shows different views of the virtual 3D reconstruction of the remaining fossilized bone after the surrounding fossilized sediment matrix and the plaster layer have been removed by means of segmentation. The multiple fracture lines, the major fracture zone (which divides the vertebral body into a ventral and dorsal half), and the destroyed anterior part of the vertebral body with the dislocated fragment in front are clearly visible.

The 3D print of the fractured fossilized bone and the fragment are depicted in Figure 8. As expected from the images, the fragmented piece fits exactly into the void of the anterior rim. The manufactured model of the vertebra is the exact physical copy of the digital reconstruction. The spatial arrangement of the fragments, as well as the surface details, is clearly visible and may be observed directly. The real unprepared fossil, with its original surrounding protective plaster jacket, and the 3D print of the segmented fossilized bone are depicted in Figure 9.

Discussion

The main aim of our study was to reveal the contents of the plaster jacket and to produce a 3D print of a fossilized bone from a CT dataset without conventional preparation. Our results demonstrate the feasibility of the methods used to nondestructively produce an actual replica of a fossilized bone without destroying the surrounding sediment.

The idea of our study is based on the combination of two methods that are already well established in the field of paleontology: CT imaging and 3D printing. For more than 30 years, CT has been used to examine fossils. Among the first studies, in 1979, Jungers and Minns (3) reported on how CT was used to compare the geometric and biomechanical properties of primate fossilized femora and tibia. Ever since, investigators have used CT for various purposes in this field, including the evaluation of patterns of paravertebral ossification in prehistoric saber-toothed cats (5), the exploration of endocranial casts of dinosaurs (6,7), and the visualization of the internal structure of pneumatized vertebrae of sauropods (8,9). Before CT was available for researchers in this field, destructive methods such as mechanical preparation were the only means with

Figure 7

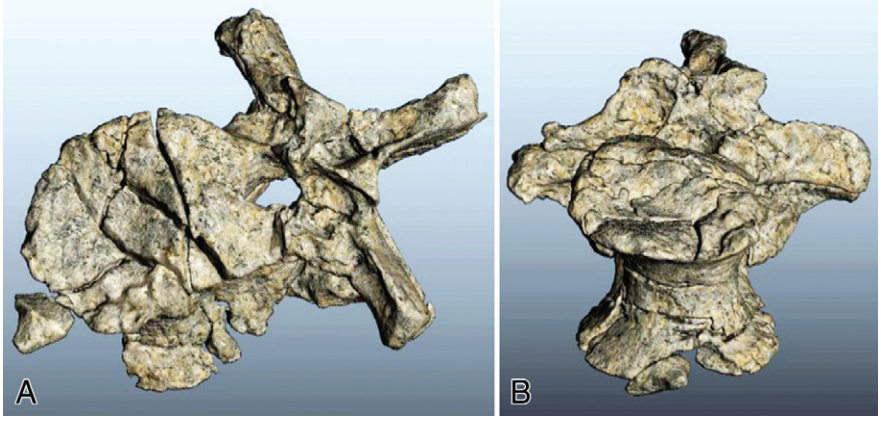

Figure 7: Virtual 3D reconstructions of fossilized vertebral body after surrounding sediment matrix and protective plaster have been digitally removed through segmentation of CT dataset. Multiple fracture lines and dislocated fragment from anterior rim of vertebral body are clearly visible.

Figure 8

Figure 8: 3D print of vertebral body.

Figure 9

Figure 9: 3D print next to the original unprepared and erroneously labeled plaster jacket.

which to gain information about fossils embedded in plaster jackets.

CT is an invaluable tool to gain fast—and, most important, nondestructive—insights into an embedded fossil. In a study performed on dinosaur eggs partially embedded in sediment, CT accurately depicted unsuspected hatching holes beneath the sediment matrix (10).

Our CT images of the fossil clearly depict a fossilized vertebral body embedded in sediment matrix. The visual identification of the vertebral body was rather easy, as its attenuation was about 450 HU higher than that of the surrounding matrix. Because of its location within the formerly collapsed basement of the Museum für Naturkunde, the original location of the specimen was unknown. However, our CT examination provided enough data to assign the fossil to the genus *Plateosaurus* from the Halberstadt excavation. *Plateosaurus* is a bipedal and presumably omnivorous sauropodomorph dinosaur with a relatively long neck, which could reach a length of up to 10 m. The genus is known from central Europe and was very common in some localities in Southern Germany, Switzerland, and Halberstadt (11). Studies of excavation maps and field lists made by preparator Siegert during the excavation of the specimens in 1927 indicate that it was not specimen A (although it was assigned field number A-48 after the war), but specimen B from the same excavation site.

In addition, much valuable information about the condition and integrity of the fossil has been gained as well, especially concerning the multiple fractures and the major fracture zone dividing the entire fossil. Furthermore, we were able to identify destruction of the anterior rim of the vertebral body with dislocated fossilized fragments. This suggests that the anterior destruction and fractures must have occurred after the fossil was packed in plaster, either during transport or possibly due to the bombing of the Museum für Naturkunde during World War II. If removal of the specimen from the plaster jacket and sediment matrix is attempted, this information will be very useful for the preparator.

Beyond CT imaging and 3D virtual reconstruction, 3D printouts of fossils have gained considerable importance in the field of paleontology. As with CT, rapid advances in technology and cheaper availability of 3D printers make it more and more common to use this method as a tool for research. One of the most important features of this method is that, while the rare original

fossil may be kept safe, digital models of the objects can be transferred rapidly among researchers and endless numbers of exact copies can be produced and distributed to colleagues, greatly advancing scientific exchange. So far, these printouts were limited to fossilized objects already separated from their surrounding sediment matrix. Our aim was to test whether it is feasible to generate an actual 3D print of an unprepared vertebral body, by virtually separating it from its surrounding matrix, with use of the CT dataset of the entire object. The CT images show that the 3D print we generated may be considered an accurate copy of the virtual 3D reconstruction. The multiple fracture lines as well as the dislocated fragment from the anterior rim are clearly visible, and thus it may be concluded that, in the future, virtual preparations with 3D printouts of fossils may be performed without having to destroy the fossil itself. Therefore, our approach may be a novel alternative to conventional methods that allows preservation of these rare objects of old excavations.

The process chain of CT scanning, segmentation, and 3D printing provides new insights into fossil objects, and full accessibility of a fossil's virtual and physical copies opens up new ways of observation, interaction, and modification. It enables damage-free scientific research, as well as global interchange of unique fossils. Furthermore, in the future, the physical representation may provide a natural 3D visual and haptic experience not only to scientists but also to a nonscientific audience.

Acknowledgments: The authors thank Martin C. Barck and Adam Brych (from 3D Laboratory, Faculty II, Institute for Mathematics, Technische Universitaet Berlin, Germany) for their outstanding support in generating the 3D print. Also we would like to thank Heinrich Mallison, Dr rer nat (from the Museum of Natural History, Leibniz Institute for Evolution and Biodiversity Research, Berlin, Germany), for providing us the illustration of Plateosaurus.

Disclosures of Conflicts of Interest: R.S. No relevant conflicts of interest to disclose. **B.J.** No relevant conflicts of interest to disclose. **O.W.** No relevant conflicts of interest to disclose. **D.S.** No relevant conflicts of interest to disclose. **A.S.I.** No relevant conflicts of interest to disclose.

References

1. Maier G. African dinosaurs unearthed: the Tendaguru expeditions. Bloomington, Ind: Indiana University Press, 2003.
2. Böhme G. Otto Jaekel und das Museum für Naturkunde der Berliner Universität. Wissenschaftliche Zeitschrift der Ernst-Moritz-Arndt-Universität Greifswald, Mathematisch-naturwissenschaftliche Reihe 1989; 38(1-2):18–21.
3. Jungers WL, Minns RJ. Computed tomography and biomechanical analysis of fossil long bones. Am J Phys Anthropol 1979;50(2):285–290.
4. Golder W, Christian A. Quantitative CT of dinosaur bones. J Comput Assist Tomogr 2002;26(5):821–824.
5. Bjorkengren AG, Sartoris DJ, Shermis S, Resnick D. Patterns of paravertebral ossification in the prehistoric saber-toothed cat. AJR Am J Roentgenol 1987;148(4):779–782.
6. Knoll F, Witmer LM, Ortega F, Ridgely RC, Schwarz-Wings D. The braincase of the basal sauropod dinosaur *Spinophorosaurus* and 3D reconstructions of the cranial endocast and inner ear. PLoS ONE 2012;7(1):e30060.
7. Knoll F, Schwarz-Wings D. Palaeoneuroanatomy of *Brachiosaurus*. Ann Paleontol 2009;95(3):165–175.
8. Wedel M. The evolution of vertebral pneumaticity in sauropod dinosaurs. J Vertebr Paleontol 2003;23(2):344–357.
9. Schwarz D, Fritsch G. Pneumatic structures in the cervical vertebrae of the late Jurassic (Kimmerigian-Tithonian) Tendaguru sauropods *Brachiosaurus brancai* and *Dicraeosaurus*. Eclogae Geol Helv 2006;99(1):65–78.
10. Jones JC, Greenberg W, Ayers MS. Computed tomographic evaluation of dinosaur egg shell integrity. Vet Radiol Ultrasound 1998;39(2):133–136.
11. Galton P, Upchurch P. Prosauropoda. In: The Dinosauria. 2nd ed. Berkeley, Calif: University of California Press, 2004.